Chaos, Solitons and Fractals 81 (2015) 432–442

Contents lists available at ScienceDirect

Chaos, Solitons and Fractals

Nonlinear Science, and Nonequilibrium and Complex Phenomena

journal homepage: www.elsevier.com/locate/chaos

Power-law statistics from nonlinear stochastic differential equations driven by Lévy stable noise

Rytis Kazakevičius, Julius Ruseckas*

Institute of Theoretical Physics and Astronomy, Vilnius University, A. Goštauto 12, Vilnius LT-01108, Lithuania

ARTICLE INFO

Article history:
Available online 19 September 2015

Keywords:
Stochastic analysis methods
Random walks and Lévy flights
1/f noise
Anomalous diffusion

ABSTRACT

Anomalous diffusion occurring in complex dynamical systems can often be described by Langevin equations driven by Lévy stable noise. Nonlinear stochastic differential equations yielding power-law steady state distribution and generating signals with $1/f$ power spectral density can be generalized by replacing the Gaussian noise with a more general Lévy stable noise. These nonlinear equations can generate signals exhibiting anomalous diffusion: either sub-diffusion or super-diffusion. In a special case when stability index is $\alpha = 2$, we retain the equations with the Gaussian noise. We investigate numerically the frequency range where the spectrum has $1/f$ form and demonstrate that this frequency range depends on power-law exponent in steady state distribution as well as on the index of stability α. We expect that this generalization may be useful for describing $1/f$ fluctuations in the complex systems exhibiting anomalous diffusion.

1. Introduction

One of the fundamental aspects of complex systems is the transport properties. Transport properties in complex systems are usually characterized by anomalous scaling, that is by a non-linear time dependency in the growth of the variance, $\sigma^2(t) \sim t^\mu$, where t is the elapsed time. This condition is known as an anomalous diffusion. In contrast to the anomalous diffusion, in a typical diffusion process the variance of the particle position (or mean squared displacement σ_x^2) is a linear function of time. Physically, the variance $\sigma^2(t)$ can be considered as the amount of space that the particle has "explored" in the system. Anomalous diffusion is classified by its power law exponent μ. If $\mu > 1$, the phenomenon is called super-diffusion. Super-diffusion has been experimentally observed in a study of tracer particles in a two-dimensional rotating flow [1]. If $\mu < 1$, the particle undergoes sub-diffusion. Sub-diffusion has been proposed as a measure of macromolecular crowding in the cytoplasm [2]. It has been theoretically shown that anomalous diffusion can arise in self-organized criticality (SOC) systems such as sandpile [3] and play important role to self-organization phenomena in reaction–diffusion systems [4].

Theoretical models suggest that super-diffusion can be caused by Lévy flights [5]. Analysis of the relaxation cascade of a photoexcited electron in graphene showed that the statistics of the entire cascade is described by Lévy flights with constant drift leading to anomalous diffusion [6]. Lévy flight is a generalization of the Brownian motion. The Brownian motion mimics the influence of the "bath" of surrounding molecules in terms of time-dependent stochastic force which is commonly assumed to be a white Gaussian noise. This assumption is compatible with the weak interactions between the particle and the bath. On the contrary, the Lévy flights describe results of strong collisions between the particle and the surrounding environment. Lévy flights resulting in a super-diffusion can be modeled by fractional Fokker–Planck equations [7] or Langevin equations with an additive Lévy stable noise. Langevin equations have been used to study the role of thermal and non-Gaussian noise

* Corresponding author. Tel.: +3705 2193256.
E-mail address: julius.ruseckas@tfai.vu.lt (J. Ruseckas).

http://dx.doi.org/10.1016/j.chaos.2015.08.024
0960-0779/

on the dynamics of driven short overdamped [8] and long-overlap Josephson junctions [9]. The resonant activation and noise enhanced stability has been observed in a metastable system in the presence of Levy noise. Lévy motions can lead to anomalous diffusion in many physical systems: as an example we mention deterministic chaotic dynamics of Na adparticles on a Cu surface [10], anomalous diffusion of a gold nanocrystal, adsorbed on the basal plane of graphite [11].

Sub-diffusion can be described with an additional assumption that diffusing particle become trapped for some times and the waiting time distribution is of a power law type. For example, assuming anomalously long waiting times $p(t) \sim 1/t^{1+m}$, $0 < m < 1$, one arrives at an anomalous, non-Markovian diffusion which is described by the fractional (in time) Fokker–Planck–Kolmogorov equation [12]. However, if it is unreasonable to assume existence of the trapping mechanism, alternative approach can be made by using models with multiplicative Lévy stable noise [13]. Langevin equations with multiplicative Lévy stable noise have been used for modeling inhomogeneous media [14] and for the description of the competition between two competing species in super-diffusive dynamical regimes. The multiplicative noise, in the presence of two different dynamical regimes (coexistence and exclusion) produces the appearance of anticorrelated oscillations and stochastic resonance phenomenon [15,16]. The relation between Langevin equation with multiplicative Lévy stable noise and fractional Fokker–Planck equation has been introduced in [17]. The Langevin equation should be interpreted in Itô sense [18]. Unfortunately the relation between these two equations is not known in Stratonovich interpretation, therefore application of Lévy stable noise driven stochastic differential equations (SDEs) can be problematic. For equation driven by Gaussian noise we can always write the corresponding Fokker–Planck equation and vice versa. However, such statement is not always true for Langevin equation with Lévy stable noise. For example, particle diffusion on randomly folding heteropolymer can be described by space fractional Fokker–Planck equation [19], but for such equation counterpart Langevin equation has not been found [20] and may not exist [21].

There are some exceptional cases when stochastic differential equations with Lévy stable noise have generated a signal with statistical properties that mimics experiment data very well, like in a study of Lévy stable noise induced millennial climate changes from an ice-core record [22]. However, the choice of appropriate model for noisy system can very difficult. In many experimental studies it is usually possible only to show that the systems exhibit Lévy law-tails: for example, distribution function of turbulent magnetized plasma emitters [23] and step-size distribution of photons in hot vapors of atoms [24] have Lévy tails. Financial data time series analysis show that other stochastic process can be indistinguishable from Lévy stable motion [25].

Many complex systems exhibit large fluctuations of macroscopic quantities having non-Gaussian power law distributions as well as power law temporal correlations and scaling [26–28]. The power law distributions, scaling, self-similarity and fractality can be related with the power law behavior of the power spectral density (PSD), that is $1/f$ noise. "$1/f$ noise" refers to signals having the PSD at low frequencies f of the form $S(f) \sim 1/f^{\beta}$ with β close to 1. Power-law spectra of signals with $0.5 < \beta < 1.5$, as well as scaling behavior are ubiquitous in physics and in many other fields [29–36]. Since its discovery more than 80 years ago [37,38] many models and theories have been proposed. Nevertheless, the subject of $1/f$ noise remains still open for new discoveries. Most models and theories of $1/f$ noise are not universal due to the usage of assumptions specific to the problem under consideration. A short categorization of the theories and models of $1/f$ noise is presented in the introduction of the paper [39], see also the review [40]. Mainly $1/f$ noise is considered as Gaussian process [41,42], but sometimes signals exhibiting $1/f$ spectrum are clearly non-Gaussian [43,44].

The simplest way to model $1/f$ noise is to use superposition of signals with Lorentzian spectra. However a wide range distribution of signal relaxation times is required [45]. A class of the models of $1/f$ noise especially relevant for understanding of complex systems involves the self-organized criticality [46–48]. Yet another model of $1/f$ has been presented in [49–52]: it has been shown that the origin of $1/f$ noise in a signal consisting from pulses may be a Brownian motion of the time between pulses. The nonlinear SDEs generating signals with $1/f$ noise has been obtained in [53,54] starting from this point process model of $1/f$ noise. It has been shown that a special case of this SDE arises from Kirman's agent model [55]. This equation was used to describe signals in socio-economical systems [56,57].

The nonlinear SDEs generating signals with $1/f$ PSD have been generalized in [58] by replacing the Gaussian noise with a more general Lévy stable noise. The SDEs with the Gaussian noise then arise as a special case when the index of stability $\alpha = 2$. The signals generated by proposed SDEs have $1/f^{\beta}$ PSD in a wide but finite region of the frequencies. The analytical estimation of the width of this region, obtained in [58] shows poor agreement with numerical results.

In this paper we numerically investigate the dependence of the width of $1/f$ region in the spectrum on the parameters of the equation. It has been shown that for noisy linear oscillator the efficiency of the noise energy conversion process depends only on the correlation time and the bandwidth of the noise [59]. We expect that knowledge of the size of $1/f$ noise frequency range will be useful for better understanding of the non-Gaussian noise energy harvesting in monostable piezoelectric transducers [60]. The power law distributions, scaling, self-similarity and fractality can be related with the $1/f$ noise and anomalous diffusion [61]. We use nonlinear SDEs with Lévy stable noise to study the connection between anomalous diffusion and $1/f$ noise.

The paper is organized as follows: In Section 2 we present the nonlinear SDE with Lévy stable noise yielding power law steady state probability density function (PDF) of the generated signal. In Section 3 we discuss the numerical method of solution. This method we apply in Section 4 to estimate when the signal generated by such an SDE has $1/f$ PSD in a wide region of frequencies. In Section 5 we explore the relation between our model and anomalous diffusion. Section 6 summarizes our findings.

2. Stochastic differential equation with Lévy stable noise generating signals exhibiting 1/*f* spectrum

We consider the Langevin equation with Lévy stable noise of the form [7,62,63]

$$\frac{dx}{dt} = a(x) + b(x)\xi(t), \tag{1}$$

where $a(x)$ describes the deterministic drift term and $b(x)$ describes the amplitude of the noise. The stochastic force $\xi(t)$ is uncorrelated white noise, $\langle \xi(t)\xi(t')\rangle = \delta(t-t')$ and is characterized by Lévy α-stable distribution. For simplicity we only use symmetric stable distributions, for this reason we take the characteristic function of $\xi(t)$ as

$$\langle \exp(ik\xi)\rangle = \exp(-\sigma^\alpha |k|^\alpha), \tag{2}$$

where σ is the scale parameter and α is the index of stability. Eq. (1) we interpret in Itô sense. The Lévy α-stable distributions arise form generalized central limit theorem and constitute the most general class of stable processes. These distributions are characterized by the index of stability $0 < \alpha \leq 2$. The Gaussian distribution corresponds to a special case when $\alpha = 2$, whereas the Lévy stable distributions have power-law tails $\sim 1/x^{1+\alpha}$ for $\alpha < 2$. There are many systems exhibiting such power law-tails: for example, distribution function of turbulent magnetized plasma emitters [23] and step-size distribution of photons in hot vapors of atoms [24] have Lévy tails; theoretical models impose that velocity distribution of particles in fractal turbulence is Lévy stable distribution [64] or at least has Lévy tails [65]. If properties of a system subjected to noise depend mainly only on large noise fluctuations, such noise intensity distributions can by approximated by Lévy stable distribution, leading to Lévy flights. Eq. (1) can also be written in the form

$$dx = a(x)dt + b(x)dL_t^\alpha, \tag{3}$$

where dL_t^α stands for the increments of Lévy α-stable motion L_t^α [25,66]. It is easier to calculate the steady state PDF of the signal x by using the space fractional Fokker–Planck equation instead of stochastic differential equation (1). The fractional Fokker–Planck equation corresponding to Eq. (1) is [17,67]

$$\frac{\partial}{\partial t}P(x,t) = -\frac{\partial}{\partial x}a(x)P(x,t) + \sigma^\alpha \frac{\partial^\alpha}{\partial |x|^\alpha} b(x)^\alpha P(x,t). \tag{4}$$

The operator $\partial^\alpha/\partial|x|^\alpha$ is the Riesz–Weyl fractional derivative. The Riesz–Weyl fractional derivative acting on the function $f(x)$ is defined by its Fourier transform [68],

$$\mathcal{F}\left[\frac{\partial^\alpha}{\partial|x|^\alpha} f(x)\right] = -|k|^\alpha \tilde{f}(k). \tag{5}$$

The SDE (1) having multiplicative noise with the power-law dependence of the noise amplitude $b(x)$ on the signal size and generating signals with the power law steady state PDF

$$P_0(x) \sim x^{-\lambda}, \tag{6}$$

has recently been proposed in Ref. [58]. The proposed equation has the form

$$dx = \sigma^\alpha \gamma x^{\alpha(\eta-1)+1}dt + x^\eta dL_t^\alpha, \tag{7}$$

where the coefficient γ is given by the equation

$$\gamma = \frac{\sin\left[\pi\left(\frac{\alpha}{2} - \alpha\eta + \lambda\right)\right]}{\sin[\pi(\alpha(\eta-1)-\lambda)]} \frac{\Gamma(\alpha\eta - \lambda + 1)}{\Gamma(\alpha(\eta-1)-\lambda+2)}. \tag{8}$$

The special case of Eq. (7) for free particle ($a(x) = 0$) with Lévy stable noise having $\alpha < 2$ has been derived from coupled continuous time random walk (CTRW) models [13], when jumping rate ν of CTRW process depends on signal intensity as $\nu(x) = x^{\alpha\eta}$, $x > 0$. It has been obtained in Ref. [58] that the power law exponent λ of the steady state PDF should take the values from the interval

$$\alpha(\eta-1) + 1 < \lambda < \alpha\eta + 1. \tag{9}$$

In fact, this condition assures that the values of the parameters in equation (8) are outside of the poles.

If $\lambda > 1$ then the steady state PDF $P_0(x)$ diverges as $x \to 0$. The requirement of the stationarity of the process leads to the necessity to restrict the diffusion in some finite interval of values. Thus the SDE (7) should be considered together with the appropriate restrictions of the diffusion. The simplest choice of restriction is provided by the reflective boundaries at $x = x_{\min}$ and $x = x_{\max}$. Nevertheless, other forms of restrictions are possible by introducing additional terms in the drift term of Eq. (7).

Eq. (7) is a generalization of the nonlinear SDE with Gaussian noise proposed in [53,54]. As a particular case, when $\alpha = 2$ then the expression (8) for the coefficient γ simplifies to $(2\eta - \lambda)$ and from Eq. (7) we get previously proposed SDE with the Gaussian noise [53,54]

$$dx = \sigma^2(2\eta - \lambda)x^{2\eta-1}dt + x^\eta dL_t^2. \tag{10}$$

According to the definition (2), the scale parameter σ differs from the standard deviation of the Gaussian noise. Another simple case is when $\alpha = 1$. For $\alpha = 1$ Eq. (7) becomes

$$dx = \sigma\cot[\pi(\lambda - \eta)]x^\eta dt + x^\eta dL_t^1. \tag{11}$$

Recently it was suggested that the non-homogeneity arising from the bath not being in an equilibrium can be described by the dependence of the diffusion coefficient on the particle coordinate x [69]. For example, if $\eta = 1/2$, Eq. (10) describes the diffusion of a Brownian particle in a medium where steady state heat transfer is present due to the difference of temperatures at the ends of the medium. The appropriate choice of γ (Eq. (8)) preserves original scaling properties of the signal as Lévy stable noise is introduced instead of Gaussian noise. Therefore, Eq. (7) should apply to Brownian motion in non-homogeneous media in presence of anomalous scaling.

2.1. Estimation of the power spectral density

The power law exponent of the PSD can be estimated by using the approximate scaling properties of the signals, as it is done in the Appendix A of Ref. [70] and in Ref. [71]. The PSD can be obtained from the autocorrelation function $C(t)$ by using Wiener–Khintchine theorem. The autocorrelation function can be calculated using the steady state PDF $P_0(x)$ and the transition probability $P(x', t|x, 0)$ [72]:

$$C(t) = \int dx \int dx'\, xx' P_0(x) P(x', t|x, 0). \tag{12}$$

The transition probability (the conditional probability that at time t the signal has value x' with the condition that at time $t = 0$ the signal had the value x) can be obtained from the solution of the fractional Fokker–Planck equation (4) with the initial condition $P(x', t = 0|x, 0) = \delta(x' - x)$.

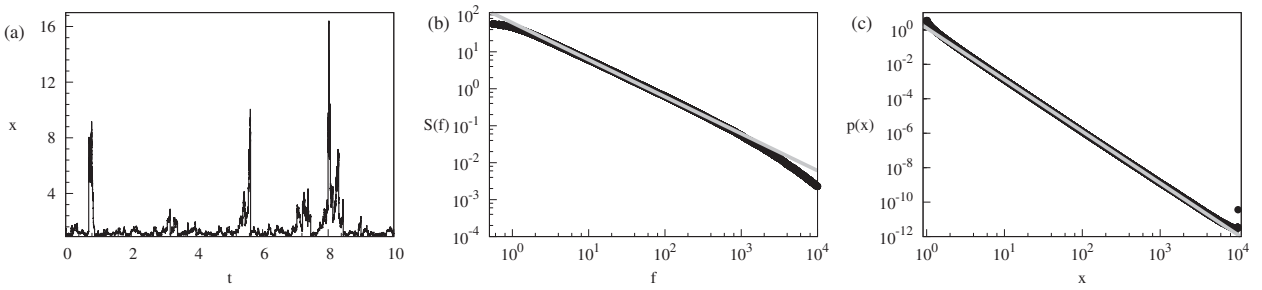

Fig. 1. (a) Signal generated by SDE with Lévy stable noise (11) with reflective boundaries at $x = x_{\min}$ and $x = x_{\max}$. (b) Steady state PDF $P_0(x)$ of the signal. The gray line shows the slope x^{-3}. (c) Power spectral density $S(f)$ of the signal. The gray line shows the slope $1/f$. Parameters used are $\alpha = 1$, $\lambda = 3$, $\eta = 1.8$, $x_{\min} = 1$, $x_{\max} = 10^4$, $\sigma = 1$.

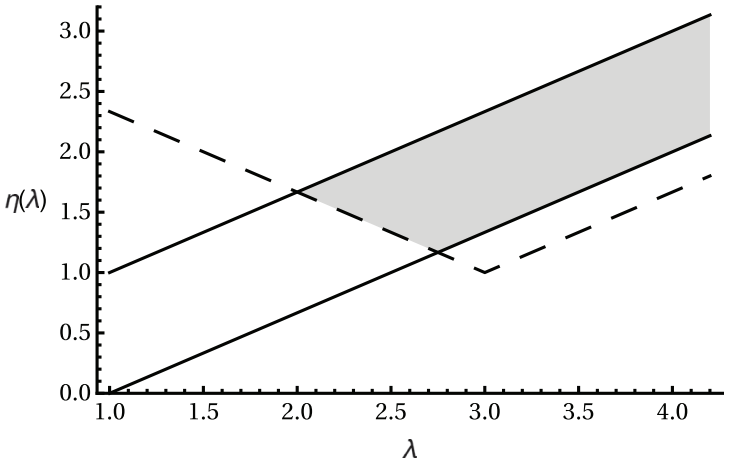

Fig. 2. Possible values of the multiplicativity parameter η and the power law exponent λ for a fixed stability index value $\alpha = 1.5$. Black solid lines represent the limiting values given by Eq. (21). The black dashed line represents the limit given by Eq. (22). The gray area represent the combination of η and λ values for which Eq. (7) generates signal with steady state distribution and power spectral density in a form of power laws.

The Lévy α-stable motion has the increments dL_t^α with the scaling property $dL_{at}^\alpha = a^{1/\alpha} dL_t^\alpha$ [66]. By introducing the scaled time $t_s = a^{\alpha(\eta-1)}t$ or changing the variable x in Eq. (7) to the scaled variable $x_s = ax$ we get the same resulting equation. Thus change of the time scale and change of the scale of the variable x are equivalent, leading to the scaling property of the transition probability

$$aP(ax', t|ax, 0) = P(x', a^\mu t|x, 0). \tag{13}$$

The exponent μ is

$$\mu = \alpha(\eta - 1). \tag{14}$$

In Ref. [71] it has been shown that the steady state PDF $P_0(x) \sim x^{-\lambda}$ and the scaling property of the transition probability (13) lead to the power law form of the PSD $S(f) \sim f^{-\beta}$ in a wide range of frequencies. The power law exponent in the PSD of the signal generated by SDE (7) is

$$\beta = 1 + \frac{\lambda - 3}{\alpha(\eta - 1)}. \tag{15}$$

This equation is valid when the resulting β has values in the interval $0 < \beta < 2$. Eq. (15) is a generalization of the expression for the power law exponent in the PSD with $\alpha = 2$ obtained in Ref. [54]. From Eq. (15) it follows that we get $1/f$ PSD when $\lambda = 3$.

Due to restrictions of diffusion at $x = x_{\min}$ and $x = x_{\max}$ the scaling (13) is not exact. This limits the power law part of the PSD to a finite range of frequencies $f_{\min} \ll f \ll f_{\max}$. Note, that pure $1/f^\beta$ PSD is physically impossible because the total power would be infinite. Therefore we consider signals with PSD having $1/f^\beta$ behavior only in some wide intermediate region of frequencies, $f_{\min} \ll f \ll f_{\max}$, whereas for small frequencies $f \ll f_{\min}$ the PSD is bounded. We can estimate the limiting frequencies similarly as in Ref. [71]. Taking into consideration the reflective boundaries $x_{\min}$ and $x_{\max}$ the autocorrelation function has the scaling property [71]

$$C(t; ax_{\min}, ax_{\max}) = a^2 C(a^\mu t, x_{\min}, x_{\max}). \tag{16}$$

From this equation it follows that time t in the autocorrelation function should enter only in combinations with the limiting values, $x_{\min}t^{1/\mu}$ and $x_{\max}t^{1/\mu}$. One can expect that the influence of the limiting values is negligible when the first combination is small and the second large. This limits the time t to the interval $\sigma^{-\alpha}x_{\max}^{\alpha(1-\eta)} \ll t \ll \sigma^{-\alpha}x_{\min}^{\alpha(1-\eta)}$. Then the frequency range where the PSD has $1/f^\beta$ behavior can be estimated as

$$\sigma^\alpha x_{\min}^{\alpha(\eta-1)} \ll 2\pi f \ll \sigma^\alpha x_{\max}^{\alpha(\eta-1)}. \tag{17}$$

Eq. (17) shows that the frequency range grows with increasing of the difference of the exponent η from 1. The frequency

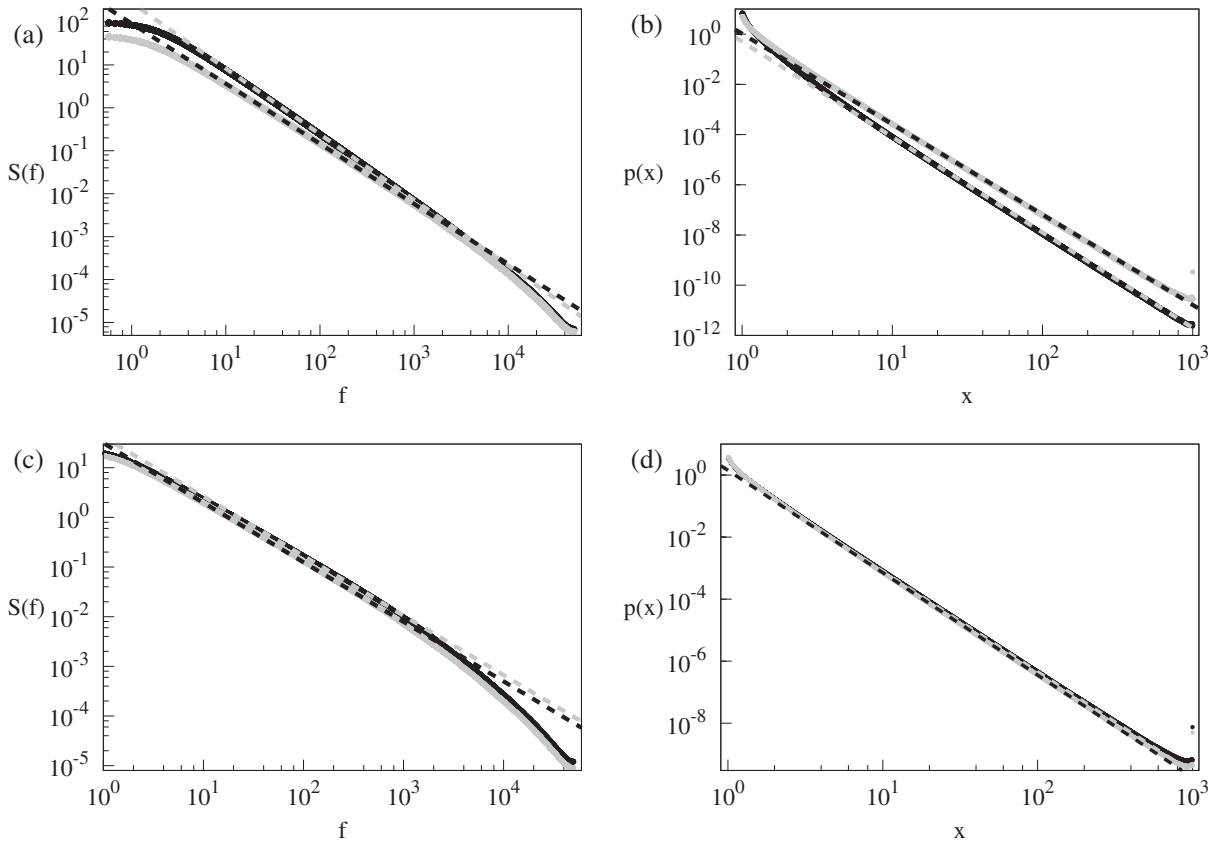

Fig. 3. (a,c) Power spectral density of signal generated by SDE with Lévy stable noise (7) and (b,d) the steady state PDF. The dashed lines show the power law dependence $1/f^{\beta}$ in (a,c) and $x^{-\lambda}$ in (b,d). The parameters are as follows: (a,b) $\lambda = 3.8$ black dots, $\lambda = 3.6$ gray dots corresponding to numerically estimated power law exponents $\beta = 1.53$ and $\beta = 1.4$. (c,d) $\lambda = 3.5$ black dots and $\lambda = 3.3$ gray dots corresponding to numerically estimated power law exponents $\beta = 1.2$ and $\beta = 1.2$. Other parameters are $x_{\min} = 1$, $x_{\max} = 10^3$, $\sigma = 1$, $\eta = 2.0$, $\alpha = 1.5$.

range becomes zero when $\eta = 1$. One can get arbitrarily wide range of the frequencies where the PSD has $1/f^{\beta}$ behavior by increasing the ratio $x_{\max}/x_{\min}$. Unfortunately, the numerical calculation shows that the estimation of the frequency range given by Eq. (17) is too wide. In order to give a better estimation we numerically investigate the dependence of the $1/f^{\beta}$ frequency range on the parameters of the equation in Section 4.

3. Method of numerical solution

It was rigorously proven by numerical simulations and algorithm convergence analysis that Euler's scheme can be used for stochastic differential equations with Lévy α stable process [66,73] and even for more complicated case when both time and space derivatives are fractional in the corresponding Fokker–Planck equation [74]. Therefore, we transform differential equations to difference equation by using Euler's approximation scheme. The difference equation

$$x_{k+1} = x_k + \sigma^{\alpha}\gamma x_k^{\alpha(\eta-1)+1} h_k + x_k^{\eta} h_k^{1/\alpha}\xi_k^{\alpha}, \tag{18}$$

corresponding to Eq. (7). We interpret the stochastic integral in Itô sense, because the relation between the Langevin equation Eq. (1) and the Fokker–Planck equation is known only in Itô interpretation. However an attempt to use Stratonovich interpretation also has been made [18]. Here $h_k = t_{k+1} - t_k$ is the discrete time step and ξ_k^{α} is a random variable having α-stable Lévy distribution with the characteristic function (2). The Eq. (18) could be solved numerically with the constant step $h_k = \text{const}$. When $\eta > 1$ the coefficients in the equation become large at large values of x, thus a very small time step is needed. It is more efficient to use a variable time step, as has been done solving SDE with Gaussian noise in Ref. [53]. We choose the time step in such a way that the change of the variable x_k in one step is proportional to the value of the variable x. If we consider the variable step of integration such as

$$h_k = \frac{\kappa^{\alpha}}{\sigma^{\alpha}} x_k^{-\alpha(\eta-1)}, \tag{19}$$

Eq. (18) simplifies to

$$x_{k+1} = x_k + \kappa^{\alpha}\gamma x_k + \frac{\kappa}{\sigma} x_k \xi_k^{\alpha}. \tag{20}$$

Here $\kappa \ll 1$ must be a small parameter. We get very similar numerical results by using the Milstein approximation.

We introduce the reflective boundaries at $x = x_{\min}$ and $x = x_{\max}$ using the projection method [75,76]. The projection method is realized as follows, if the variable x_{k+1} acquires the value outside of the interval $[x_{\min}, x_{\max}]$ then the value of the nearest reflective boundary is assigned to x_{k+1}.

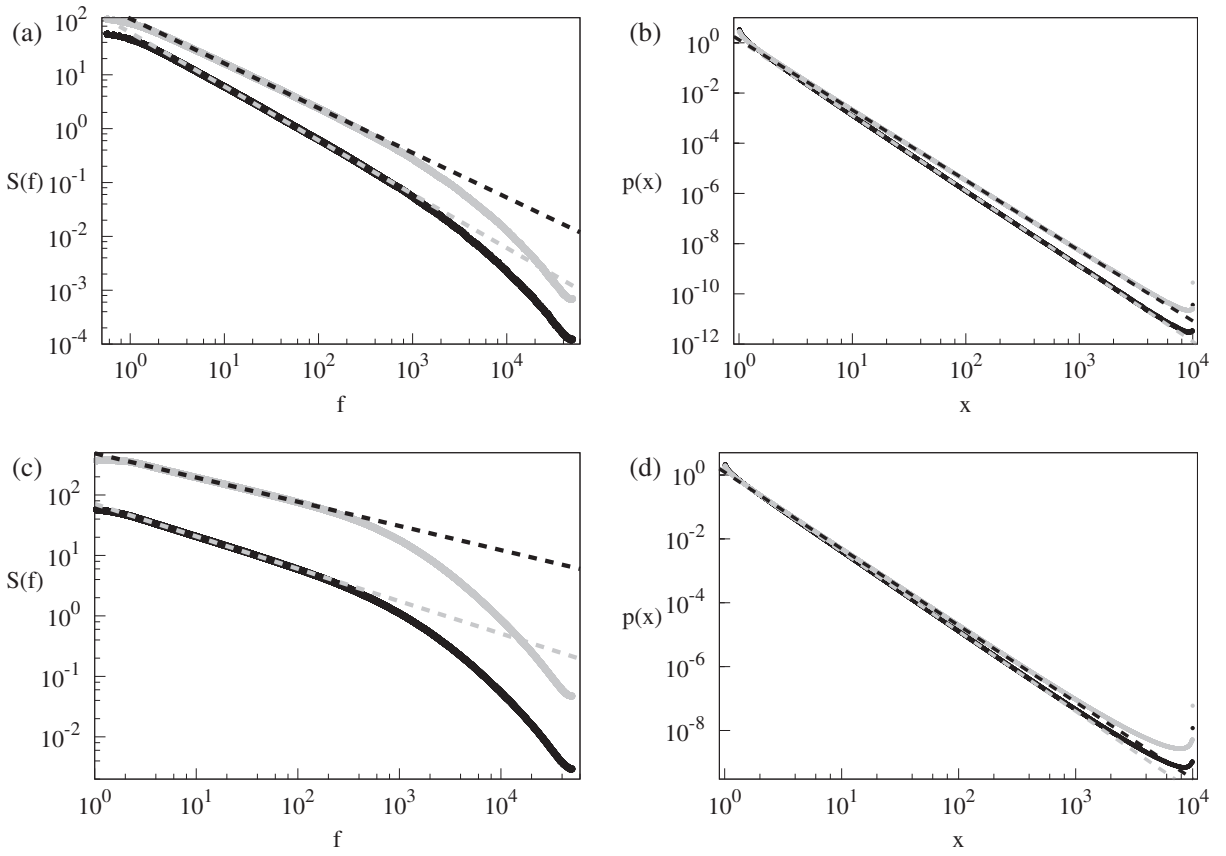

Fig. 4. (a,c) Power spectral density of signal generated by SDE with Lévy stable noise (7) and (b,d) the steady state PDF. The dashed lines show the power law dependence $1/f^{\beta}$ in (a,c) and $x^{-\lambda}$ in (b,d). The parameters are as follows: (a,b) $\lambda = 3$ black dots, $\lambda = 2.8$ gray dots corresponding to numerically estimated power law exponents $\beta = 1$ and $\beta = 0.83$. (c,d) $\lambda = 2.5$ black dots and $\lambda = 2.4$ gray dots corresponding to numerically estimated power law exponents $\beta = 0.54$ and $\beta = 0.4$. Parameters used are $x_{\max} = 10^4$, $\eta = 1.8$, other parameters are the same as used in Fig. 3.

When $\lambda = 3$, we get that $\beta = 1$ and SDEs (7), (10), and (11) should give a signal exhibiting $1/f$ fluctuations. As an example, we will solve numerically the SDE (7) with the index of stability of Lévy stable noise $\alpha = 1.5$ and the exponent of the steady state PDF $\lambda = 3$. In addition, we include the reflective boundaries at $x = x_{\min}$ and $x = x_{\max}$. The numerical results are presented in Fig. 1. We use a variable step integration sampled on constant time step equal to 10^{-5}. The generated signal is shown in Fig. 1a. In the signal we can see large peaks or bursts corresponding to the large deviations of the variable x. Comparison of the steady state PDF $P_0(x)$ with the analytical power law estimation $\sim x^{-3}$ is shown in Fig. 1b. The steady state PDF deviates from the power law prediction near reflecting boundaries. Such increase of the steady state PDF near boundaries is typical for equations with Lévy stable noise having $\alpha < 2$ [77] and is similar to the behavior of the analytical expression obtained in Ref. [77] for the simplest stochastic differential equation Lévy stable noise having constant noise amplitude and zero drift.

Comparison of the PSD $S(f)$ with the analytical estimation $S(f) \sim 1/f$ is shown in Fig. 1c. This comparison confirms the presence of the frequency region for which the PSD has $1/f$ dependence. The width of this region increases as increase the ratio between the minimum and the maximum values of the stochastic variable x. Furthermore, the region in the PSD with the power law behavior depends on α and the exponent η: the width increases with increasing the difference $\eta - 1$ and increasing α; when $\eta = 1$ then this width is zero. Such behavior is quantitatively predicted by Eq. (17). However, Eq. (17) predicts too wide frequency range. We investigate the power law frequency range dependence on model parameters in the next section.

4. Dependence of the power law region in the spectrum on the parameters of the equation

In order to investigate the dependence of the power law region in the PSD of the generated signal on the parameters of the SDE (7) we perform numerical solutions of SDEs with different power law exponents λ of steady state PDF. Extensive study of various empirical data [78] shows that power law distributions are found with power law exponent varying in interval $1.7 \leq \lambda \leq 3.7$, except some exotic cases such as the distributions numbers of papers authored by mathematicians where $\lambda = 4.3$. Therefore, we choose to vary the exponent λ in the interval $2.4 \leq \lambda \leq 3.8$.

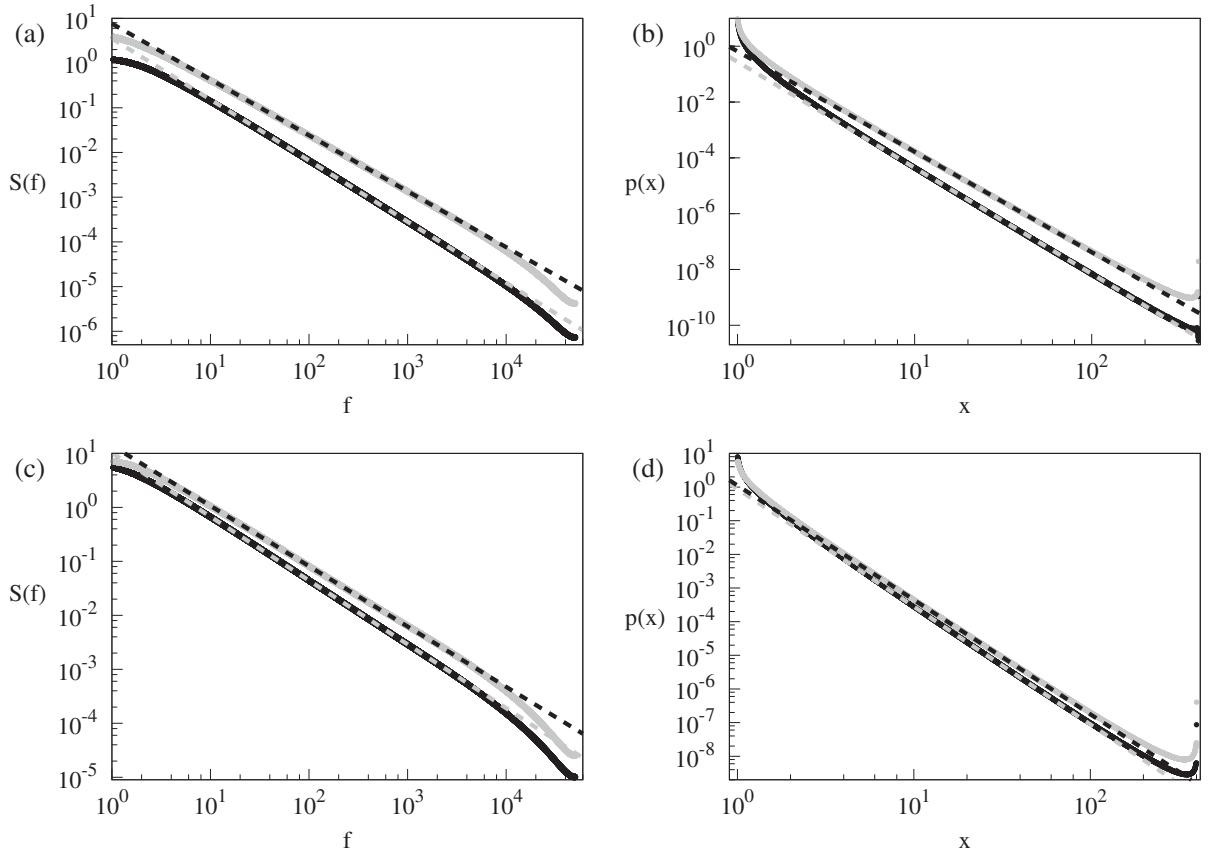

Fig. 5. (a,c) Power spectral density of signal generated by SDE with Lévy stable noise (7) and (b,d) the steady state PDF. The dashed lines show the power law dependence $1/f^{\beta}$ in (a,c) and $x^{-\lambda}$ in (b,d). The parameters are as follows: (a,b) $\lambda = 3.8$ black dots, $\lambda = 3.6$ gray dots corresponding to numerically estimated power law exponents $\beta = 1.37$ and $\beta = 1.25$. (c,d) $\lambda = 3.5$ black dots and $\lambda = 3.3$ gray dots corresponding to numerically estimated power law exponents $\beta = 1.18$ and $\beta = 1.02$. Other parameters are $x_{\min} = 1$, $x_{\max} = 400$, $\sigma = 1$, $\eta = 3.0$, $\alpha = 1$.

According to Eq. (9), the parameter η can acquire values from the interval

$$\frac{\lambda - 1}{\alpha} < \eta < \frac{\lambda - 1}{\alpha} + 1 \tag{21}$$

assuming that $\eta > 1$. On the other hand, Eq. (15) together with the condition $0 < \beta < 2$ yield

$$\eta > 1 + \frac{|\lambda - 3|}{\alpha}. \tag{22}$$

Fig. 2 shows the possible values of η and λ for fixed stability index α. The inequalities given by Eqs. (21) and (22) can be simultaneously satisfied only when $\lambda > 2$. Therefore, we expect that Eq. (15) should be valid only for $\lambda > 2$. It can be shown that for large power law exponent $\lambda > (4+\alpha)/2$ it is enough to only check the first condition Eq. (21). For smaller $\lambda < (4+\alpha)/2$ we have the interplay between limiting conditions and η can acquire values from interval

$$1 + \frac{3 - \lambda}{\alpha} < \eta < 1 + \frac{\lambda - 1}{\alpha} \tag{23}$$

This limiting range for η vanishes as $\lambda \to 2$. As an example, the PSD and the steady state PDF of the signal generated by the nonlinear SDE with Lévy stable noise and different values of the power law exponent of the steady state PDF λ are presented in Figs. 3 and 4. The index of stability is the same and equal to $\alpha = 1.5$. We see a good agreement of the steady state PDF with the analytical estimation $x^{-\lambda}$, except near the reflecting boundaries. Numerical solution of Eq. (7) confirms the presence of the frequency region where the PSD has $1/f^{\beta}$ dependence. From the condition Eq. (9) and Eq. (15) it follows that Eq. (7) should yield power law PSD with the exponent β having values from the interval

$$2 - \frac{2}{\alpha(\eta - 1)} < \beta < 2 - \frac{2 - \alpha}{\alpha(\eta - 1)} \tag{24}$$

when $\eta > 1$. However, numerical calculation shows that for $2 < \lambda < 2.5$ Eq. (15) does not hold precisely. For example, Eq. (15) with the parameters corresponding to Fig. 4c gives $\beta = 0.5$, but numerical simulation yields $\beta = 0.41$. We can conclude, that Eq. (15) is only approximate, the difference from the actual value of β becomes large when η is close to the limiting values. This is true for all λ values if η is chosen close to its limiting value. When λ is close to 2, the noise multiplicativity parameter η is always close to its limiting values and it is not possible to choose otherwise (see Fig. 2 and Eq. (23)). For larger $\lambda > 2.5$ we choose η sufficiently far from limiting values. Therefore for $\lambda > 2.5$ the agreement of the numerical results with the analytical expressions is quite good. The analytical predictions fails close to limiting values because normalization constant γ in Eq. (7) is only

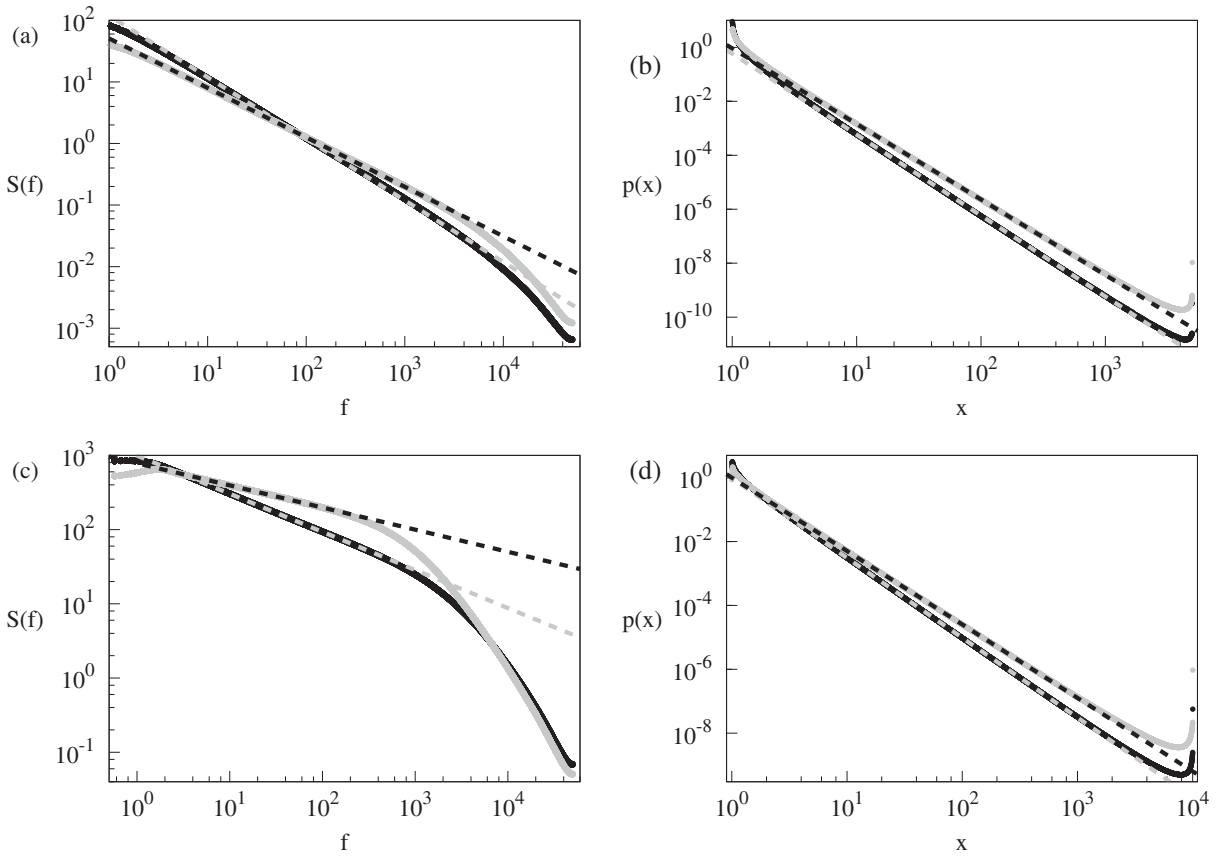

Fig. 6. (a,c) Power spectral density of signal generated by SDE with Lévy stable noise (7) and (b,d) the steady state PDF. The dashed lines show the power law dependence $1/f^{\beta}$ in (a,c) and $x^{-\lambda}$ in (b,d). The parameters are as follows: (a,b) $\eta = 2.4$, $x_{\max} = 5 \times 10^3$, $\lambda = 3$ black dots, $\lambda = 2.8$ gray dots. The corresponding numerically estimated power law exponents are $\beta = 1$ and $\beta = 0.8$. (c,d) $\eta = 2.2$, $\eta = 2.2$, $x_{\max} = 10^4$, $\lambda = 2.5$ black dots and $\lambda = 2.3$ gray dots. The corresponding numerically estimated power law exponents are $\beta = 0.51$ and $\beta = 0.3$. Other parameters are the same as used in Fig. 5.

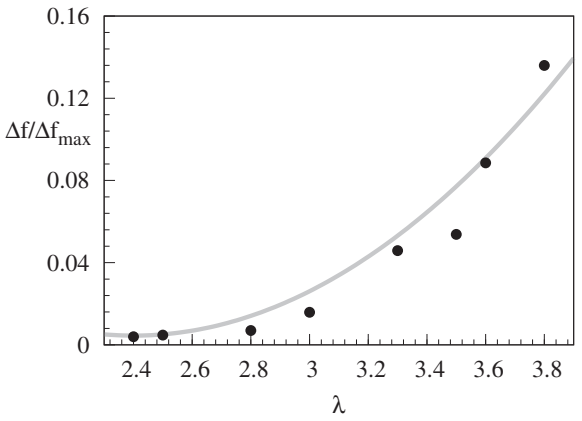

Fig. 7. Dependence of the ratio of the widths of numerical Δf_{num} and theoretical $\Delta f_{\max}$ frequency ranges where the PSD has power law behavior on the power law exponent of the steady state PDF λ. The index of stability $\alpha = 1.5$. Black dots are obtained using frequency ranges from data presented in Figs. 3 and 4. Gray line shows quadratic dependence on λ.

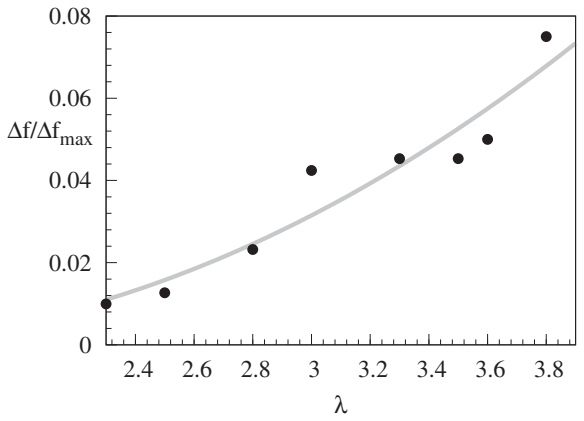

Fig. 8. Dependence of the ratio of the widths of numerical Δf_{num} and theoretical $\Delta f_{\max}$ frequency ranges where the PSD has power law behavior on the power law exponent of the steady state PDF λ. The index of stability $\alpha = 1$. Black dots are obtained using frequency ranges from data presented in Figs. 5 and 6. Gray line shows quadratic dependence on λ.

approximate when model parameters are close to the limiting values. We suspect that this happens due simplifications made in order to obtain steady state solution of fractional Fokker–Planck equation [58].

The PSD and the steady state PDF of the signal generated by the nonlinear SDE with Lévy stable noise having index of stability $\alpha = 1$ are presented in Figs. 5 and 6. The numerical solution of Eq. (11) also confirms the presence of $1/f^{\beta}$ spec-

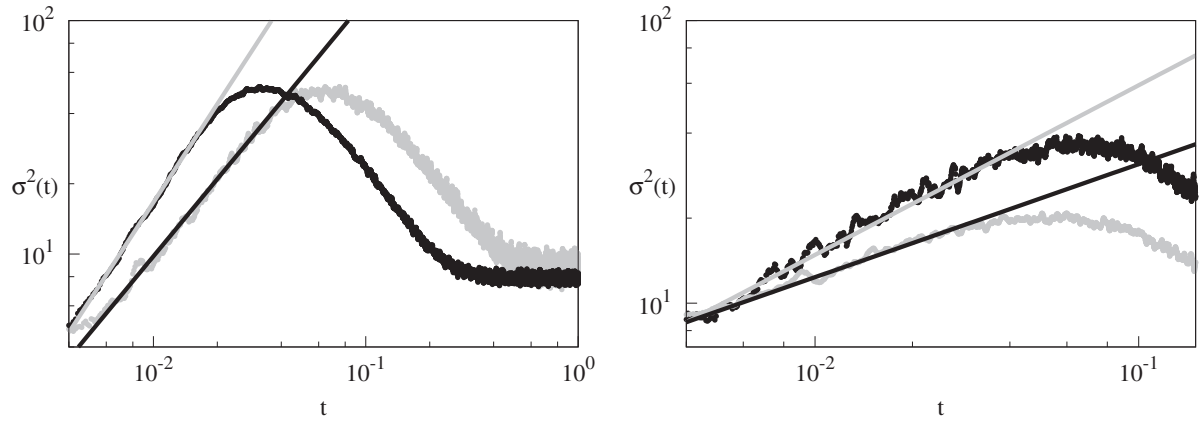

Fig. 9. Dependence of the variance $\sigma^2(t)$ of the signal generated by Eq. (7) on time t. Gray and black strait lines show the power law dependence of the variance on time, $\sigma^2 \sim t^\mu$. (a) Super-diffusive behavior when the stability index of Lévy noise $\alpha = 1.5$. Black curve corresponds to $\eta = 2.1$, gray curve to $\eta = 1.9$. The numerically determined values of the index μ are $\mu = 1.4$ and $\mu = 1.1$, respectively. (b) Sub-diffusive behavior when the stability index of Lévy noise $\alpha = 1.2$. Black curve corresponds to $\eta = 2.1$, gray curve to $\eta = 1.9$. The numerically determined values of the index μ are $\mu = 0.6$ and $\mu = 0.4$, respectively. Other parameters of the equation are $\lambda = 3$, $x_{\min} = 1$, $x_{\max} = 10^4$, $\sigma = 1$.

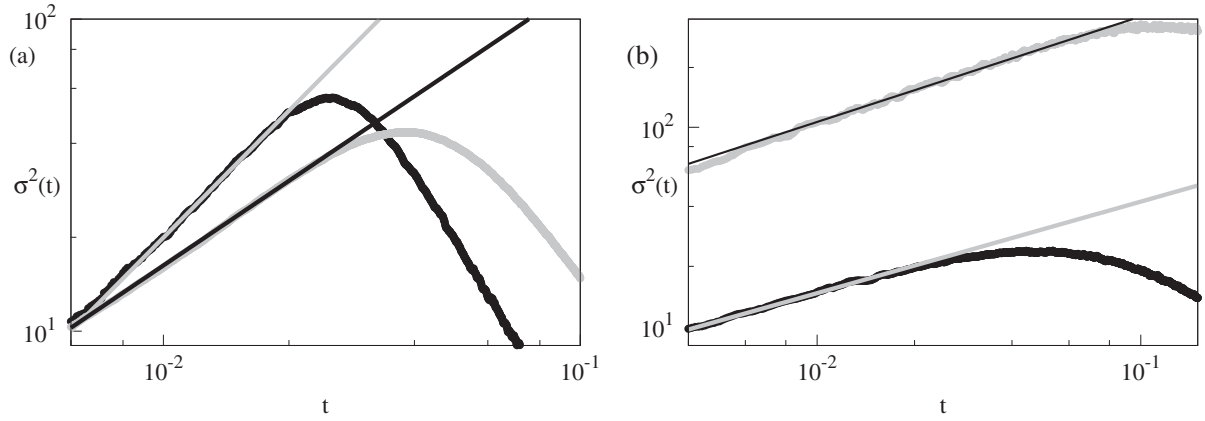

Fig. 10. Dependence of the variance $\sigma^2(t)$ of the signal generated by Eq. (11) on time t. The stability index of Lévy noise $\alpha = 1$. Gray and black strait lines show the power law dependence of the variance on time, $\sigma^2 \sim t^\mu$. (a) Black curve corresponds to $\eta = 2.8$, gray curve to $\eta = 2.9$. The numerically determined values of the index μ are $\mu = 1.35$ and $\mu = 0.9$, respectively. (b) Black curve corresponds to $\eta = 2.4$, gray curve to $\eta = 2.1$. The numerically determined values of the index μ are $\mu = 0.5$. Other parameters of the equation are same as in Fig. 9.

trum. However, as we can see from Figs. 5 and 6, the difference between the numerically obtained values of the exponent β and the values calculated using Eq. (15) is larger compared to $\alpha = 1.5$ case. The value given by Eq. (15) exactly coincides with the numerical value only in the case of pure $1/f$ noise, when $\lambda = 3$. The agreement of the steady state PDF with the power law form $x^{-\lambda}$ is much better, in all cases the power law exponent λ of the steady state PDF is equal to its theoretical value.

We numerically investigate also the width Δf_{num} of $1/f^\beta$ region in the PSD. Due to restrictions Eq. (9) the parameter η must be changed slightly by changing λ. We eliminate the dependence of Δf_{num} on the noise multiplicativity exponent η by dividing the width Δf_{num} by the width $\Delta f_{\max} = f_{\max} - f_{\min}$, where the limiting frequencies $f_{\min}$ and $f_{\max}$ are given by Eq. (17). The dependence of the ratio $\Delta f_{\text{num}}/\Delta f_{\max}$ on the power law exponent of the steady state PDF λ are presented in Fig. 7 for $\alpha = 1.5$ and in Fig. 8 for $\alpha = 1$. As the numerical results show, the actual width of the power law region in the PSD depends on the exponent λ of the steady state PDF, in contrast to the estimation given by Eq. (17). For the noise stability index $\alpha = 1.5$ the ratio $\Delta f_{\text{num}}/\Delta f_{\max}$ has a quadratic dependence on the exponent λ. For $\alpha = 1$ the points are dispersed in Fig. 8, but the quadratic dependence still can be seen.

5. Connection to anomalous diffusion

In this Section we numerically investigate the dependence of the variance $\sigma^2(t)$ on time t. In this paper we are only concerned about case when $1/f$ noise and anomalous diffusion occur together. Anomalous scaling can appear for similar SDEs that do not exhibit $1/f$ noise if the steady state PDF has a power law tail [14]. Numerical solution of SDEs (7) show that for small enough times the dependence of the variance on time can be described by a power law t^μ. According to the most common definition of anomalous diffusion [5], anomalous diffusion is a diffusion process with non-linear

time dependency in the growth of the variance.

$$\sigma^2(t) = \langle [x(t) - \langle x(t) \rangle]^2 \rangle \sim t^{\mu}. \quad (25)$$

Unfortunately the second moment of the Lévy process is divergent $\langle x^2_{\text{Levy}} \rangle = \infty$ for all times and even the mean is divergent for some cases. It has been proposed [5] to use fractional moments to analyze anomalous diffusion caused by Lévy flights, Therefore a fractional moments $\langle |x|^{\delta} \rangle$ was introduced to describe diffusion. These fractional moments are finite for all times if condition $0 < \delta < \alpha$ is satisfied. However, first and second moments are divergent only for an unbounded Lévy flight. The SDE driven by Lévy process can generate signals with finite moments if an external potential is introduced or some appropriate boundary conditions are assumed.

A general analytical expression for steady state PDF in the case of fractional Fokker–Planck equation is not known. Therefore it is hard to find such an additional drift term that limits the size of the jumps, but does not change the power law dependence of the steady state PDF in some bounded region $x \in [x_{\min}, x_{\max}]$. Thus instead of an external potential we choose to use reflective boundary conditions at $x_{\min}$ and $x_{\max}$.

We have calculated the variance taking the signal of 10^5 realizations generated by SDEs (7) and (11). For computing the variance we use an incremental algorithm [79]. The dependence of the variance σ^2 on time t for various choices of parameters is shown in Figs. 9 and 10. As we can see the power-law growth of variance is observable only for short times (approximately for 10^{-2}–10^{-1}). Due to reflective boundary conditions the variance stops growing and relax to its steady value. We determine the exponent μ describing the growth of the variance with time by fitting the initial part of time dependence to a straight line in a double logarithmic plot. We see that the power law exponent μ describing the growth of the variance with time depends on the stability index of Lévy noise α and on the noise multiplicativity exponent η. The exponent μ increases with increasing of the noise multiplicativity exponent η. For large values of η super-diffusion occurs ($\mu > 1$), for smaller values of η the sub-diffusion takes place. The value of η corresponding to the normal diffusion and thus making the boundary between the two regimes depends on the stability index α.

This dependence of the exponent μ on the noise multiplicativity exponent η we show in more detail in Fig. 10. As can be seen in Fig. 10a, the super-diffusion can be obtained for $2.8 \leq \eta < 3$. For $2.5 \leq \eta < 2.8$ we have the sub-diffusion with the exponent μ proportional to η. For $\eta < 2.5$ the exponent μ is almost independent from η and varies around $\mu = 0.5$, as can be seen in Fig. 10b.

6. Conclusions

We have proposed nonlinear stochastic differential equations driven by Lévy noise that generate signals exhibiting power law statistical properties: power law steady state PDF and power law spectrum in a wide range of frequencies. In addition, such nonlinear SDEs can lead to Lévy flights with anomalous diffusion, both sub-diffusion and super-diffusion. However, we were unable to find an analytical relation between the parameters of the SDE η and α and the exponent of the anomalous diffusion μ, introduced by Eq. (25). Therefore we have used numerical solution of the SDE to estimate this exponent. The numerical results show that due to presence of the multiplicative noise in SDEs both sub-diffusion and super-diffusion can occur. This is in contrast to the equations with additive noise, when only sub-diffusion is possible unless more complex non-Markovian models are used [5]. Anomalous scaling can appear for similar SDEs that do not exhibit $1/f$ noise if steady state distribution still has power law tails [14]. In this paper we investigated the situation when $1/f^{\beta}$ noise and anomalous diffusion occur together.

The analytical estimation (17) of the frequency range where the spectrum has $1/f^{\beta}$ behavior does not coincide with the numerical calculations. In this paper we numerically investigate how this frequency range depends on the parameters of the SDE. We show that, in contrast to Eq. (17), the width of this frequency range depends not only on the exponent of the multiplicative noise η but also on the power law exponent of the steady state distribution λ.

Nonlinear SDEs with Lévy noise similar to Eq. (10) have been used to investigate the wide-spectrum energy harvesting out of colored fluctuations in monostable piezoelectric transducers [60]. The system has been modeled as a linear oscillator disturbed by $1/f^{\beta}$ noise. It has been shown that for noisy linear oscillator the efficiency of the noise energy conversion process depends only on the correlation time and the bandwidth of the noise and not on the noise amplitude [59]. We expect that knowledge of the size of $1/f$ noise frequency range bandwidth can be useful for various applications for such noisy electronic circuits.

References

[1] Solomon TH, Weeks ER, Swinney HL. Observation of anomalous diffusion and lévy flights in a two-dimensional rotating flow. Phys Rev Lett 1993;71:3975.
[2] Weiss M, Elsner M, Kartberg F, Nilsson T. Anomalous subdiffusion is a measure for cytoplasmic crowding in living cells. Biophys J 2004;87:3518.
[3] Carreras BA, Lynch VE, Newman DE, Zaslavsky GM. Anomalous diffusion in a running sandpile model. Phys Rev E 1999;60:4770.
[4] Datsko BY, Gafiychuk VV. Self-organization phenomena in reaction–diffusion systems with non-integer order time derivatives. Phys Scr 2009;136:014027.
[5] Metzler R, Klafter J. The random walk's guide to anomalous diffusion: a fractional dynamics approach. Phys Rep 2000;339:1–77.
[6] Briskot U, Dmitriev IA, Mirlin AD. Relaxation of optically excited carriers in graphene: anomalous diffusion and Lévy flights. Phys Rev B 2014;89:075414.
[7] Fogedby HC. Lévy flights in random environments. Phys Rev Lett 1994;73:2517.
[8] Augello G, Valenti D, Spagnolo B. Non-Gaussian noise effects in the dynamics of a short overdamped Josephson junction. Eur Phys J B 2010;78:225.
[9] Valenti D, Guarcello C, Spagnolo B. Switching times in long-overlap Josephson junctions subject to thermal fluctuations and non-Gaussian noise sources. Phys Rev E 2014;89:214510.
[10] Guantes R, Vega JL, Miret-Artés S. Chaos and anomalous diffusion of adatoms on solid surfaces. Phys Rev B 2001;64:245415.
[11] Luedtke WD, Landman U. Slip diffusion and Lévy flights of an adsorbed gold nanocluster. Phys Rev Lett 1999;82:3835.
[12] Zaslavsky GM. Fractional kinetic equation for Hamiltonian chaos. Physica D 1994;76:110.
[13] Srokowski T, Kaminska A. Diffusion equations for a Markovian jumping process. Phys Rev E 2006;74:021103.
[14] Srokowski T. Fractional Fokker–Planck equation for Lévy flights in nonhomogeneous environments. Phys Rev E 2009;79:040104(R).

[15] La Cognata A, Valenti D, Dubkov AA, Spagnolo B. Dynamics of two competing species in the presence of Levy noise sources. Phys Rev E 2010;82:011121.
[16] Cognata AL, Valenti D, Spagnolo B, Dubkov A. Two competing species in super-diffusive dynamical regimes. Eur Phys, J B 2010;77:273.
[17] Schertzer D, Larchev M, Duan J, Yanovsky VV, Lovejoy S. Fractional Fokker–Planck equation for nonlinear stochastic differential equations driven by non-Gaussian Lévy stable noises. J Math Phys 2001;42:200.
[18] Srokowski T. Multiplicative Lévy processes: Itô versus Stratonovich interpretation. Phys Rev E 2009;80:051113.
[19] Brockmann D, Geisel T. Particle dispersion on rapidly folding random heteropolymers. Phys Rev Lett 2003;91:048303.
[20] Brockmann D, Sokolov I. Lévy flights in external force fields: from models to equations. Chem Phys 2002;284:409.
[21] Brockmann D, Geisel T. Lévy flights in inhomogeneous media. Phys Rev Lett 2003;90:170601.
[22] Ditlevsen PD. Observation of α-stable noise induced millennial climate changes from an ice-core record. Geophys Res Lett 1999;26:1441.
[23] Marandet Y, Capes H, Godbert-Mouret L, Guirlet R, Koubiti M, Stamm R. A spectroscopic investigation of turbulence in magnetized plasmas. Commun Nonlinear Sci Commun 2003;8:469.
[24] Mercadier N, Guerin W, Chevrollier M, Kaiser R. Lévy flights of photons in hot atomic vapours. Nat Phys 2009;5:602.
[25] Weron A, Burnecki K, Mercik S, Weron K. Complete description of all self-similar models driven Lévy stable noise. Phys Rev E 2005;71:016113.
[26] Mandelbrot BB. Multifractals and 1/*f* noise: wild self-affinity in physics. New York: Springer-Verlag; 1999.
[27] Mantegna RN, Stanley HE. An introduction to econophysics: correlations and complexity. Cambridge: Cambridge University Press; 2001.
[28] Lowen SB, Teich MC. Fractal-based point processes. New York: Wiley-Interscience; 2005.
[29] Ward LM, Greenwood PE. 1/*f* noise. Scholarpedia 2007;2(12):1537.
[30] Weissman MB. 1/*f* noise and other slow, nonexponential kinetics in condensed matter. Rev Mod Phys 1988;60:537.
[31] Barabasi AL, Albert R. Emergence of scaling in random networks. Science 1999;286:509.
[32] Gisiger T. Scale invariance in biology: coincidence or footprint of a universal mechanism? Biol Rev 2001;76:161.
[33] Wagenmakers E-J, Farrell S, Ratcliff R. Estimation and interpretation of $1/f^{\alpha}$ noise in human cognition. Psychon Bull Rev 2004;11:579.
[34] Szabo G, Fath G. Evolutionary games on graphs. Phys Rep 2007;446:97.
[35] Castellano C, Fortunato S, Loreto V. Statistical physics of social dynamics. Rev Mod Phys 2009;81:591.
[36] Paladino E, Galperin YM, Falci G, Altshuler BL. 1/*f* noise: implications for solid-state quantum information. Rev Mod Phys 2014;86:361.
[37] Johnson JB. The Schottky effect in low frequency circuits. Phys Rev 1925;26:71.
[38] Schottky W. Small-shot effect and flicker effect. Phys Rev 1926;28:74.
[39] Kaulakys B, Alaburda M. Modeling scaled processes and $1/f^{\beta}$ noise using nonlinear stochastic differential equations. J Stat Mech 2009;2009:P02051.
[40] Balandin AA. Low-frequency 1/*f* noise in graphene devices. Nature Nanotechnol 2013;8:549.
[41] Kogan S. Electronic noise and fluctuations in solids. Cambrige Univ. Press; 2008.
[42] Li M, Zhao W. On 1/*f* noise. Math Probl Eng 2012;2012:23.
[43] Orlyanchik V, Weissman MB, Torija MA, Sharma M, Leighton C. Strongly inhomogeneous conduction in cobaltite films: non-Gaussian resistance noise. Phys Rev B 2008;78:094430.
[44] Melkonyan SV. Non-Gaussian conductivity fluctuations in semiconductors. Physica B 2010;405:379.
[45] Kingston RH, editor. Semiconductor surface physics. Philadelphia: University of Pennsylvania Press; 1957.
[46] Bak P, Tang C, Wiesenfeld K. Self-organized criticality: an explanation of the 1/*f* noise. Phys Rev Lett 1987;59:381.
[47] Jensen HJ, Christensen K, Fogedby HC. 1/*f* noise, distribution of lifetimes, and a pile of sand. Phys Rev B 1989;40:7425.
[48] Kertesz J, Kiss LB. The noise spectrum in the model of self-organised criticality. J Phys A: Math Gen 1990;23:L433.
[49] Kaulakys B, Meškauskas T. Modeling 1/*f* noise. Phys Rev E 1998;58:7013.
[50] Kaulakys B. Autoregressive model of 1/*f* noise. Phys Lett A 1999;257:37.
[51] Kaulakys B. On the intrinsic origin of 1/*f* noise. Microelectron Reliab 2000;40:1787.
[52] Kaulakys B, Gontis V, Alaburda M. Point process model of 1/*f* noise vs a sum of Lorentzians. Phys Rev E 2005;71:051105.
[53] Kaulakys B, Ruseckas J. Stochastic nonlinear differential equation generating 1/*f* noise. Phys Rev E 2004;70:020101(R).
[54] Kaulakys B, Ruseckas J, Gontis V, Alaburda M. Nonlinear stochastic models of 1/*f* noise and power-law distributions. Physica A 2006;365:217.
[55] Ruseckas J, Kaulakys B, Gontis V. Herding model and 1/*f* noise. EPL 2011;96:60007.
[56] Gontis V, Ruseckas J, Kononovicius A. A long-range memory stochastic model of the return in financial markets. Physica A 2010;389:100–6.
[57] Mathiesen J, Angheluta L, Ahlgren PTH, Jensen MH. Excitable human dynamics driven by extrinsic events in massive communities. PNAS 2013;110:17259.
[58] Kazakevičius R, Ruseckas J. Lévy flights in inhomogeneous environments and 1/*f* noise. Physica A 2014;411:95.
[59] Méndez V, Campos D, Horsthemke W. Efficiency of harvesting energy from colored noise by linear oscillators. Phys Rev E 2013;88:022124.
[60] Deza JI, Deza RR, Wio HS. Wide-spectrum energy harvesting out of colored Lévy-like fluctuations, by monostable piezoelectric transducers. EPL 2012;100:38001.
[61] Sornette D. Critical phenomena in natural sciences, chaos, fractals, self organization and disorder: concepts and tools. Berlin: Springer-Verlag; 2006.
[62] Fogedby HC. Langevin equations for continuous time Lévy flights. Phys Rev E 1994;50:1657.
[63] Fogedby HC. Lévy flights in quenched random force fields. Phys Rev E 1998;58:1690.
[64] Takayasu H. Stable distribution and Lévy process in fractal turbulence. Prog Theor Phys 1984;72:471.
[65] Min IA, Mezic I, Leonard A. Lévy stable distributions for velocity and velocity difference in systems of vortex elements. Phys Fluids 1996;8:1169.
[66] Janicki A, Weron A. Simulation and chaotic behaviour of α - stable stochastic processes. New York: Marcel Dekker; 1994.
[67] Ditlevsen PD. Anomalous jumping in a double-well potential. Phys Rev E 1999;60:172.
[68] Samko SG, Kilbas AA, Marichev OI. Fractional integrals and derivatives: theory and applications. New York: Gordon and Breach; 1993.
[69] Kazakevičius R, Ruseckas J. Power law statistics in the velocity fluctuations of Brownian particle in inhomogeneous media and driven by colored noise. J Stat Mech 2015;2015:P02021.
[70] Ruseckas J, Kaulakys B. Intermittency in relation with 1/*f* noise and stochastic differential equations. Chaos 2013;23:023102.
[71] Ruseckas J, Kaulakys B. Scaling properties of signals as origin of 1/*f* noise. J Stat Mech 2014:P06005.
[72] Gardiner CW. Handbook of stochastic methods for physics, chemistry and the natural sciences. Berlin: Springer-Verlag; 2004.
[73] Janicki A, Weron A. Can One See α-Stable Variables and Processes? Statist. Sci. 1994;9(1):109–26.
[74] Magdziarz M, Weron A. Competition between subdiffusion and Lévy flights: a monte carlo approach. Phys Rev E 2007;75:056702.
[75] Liu YJ. Discretization of a class of reflected diffusion processes. Math Comput Simul 1995;38:103–8.
[76] Pettersson R. Approximations for stochastic differential equations with reflecting convex boundaries. Stoch Processes Appl 1995;59:295–308.
[77] Denisov SI, Horsthemke W, Hänggi P. Steady-state Lévy flights in a confined domain. Phys Rev E 2008;77:061112.
[78] Clauset A, Shalizi CR, Newman MEJ. Power-law distributions in empirical data. SIAM Rev 2009;51:661.
[79] Knuth DE. The art of computer programming. Seminumerical algorithms, 2. 3rd. Boston: Addison-Wesley; 1998.